Advances in Concrete Construction, *Vol. 14, No. 2 (2022) 79-92*
https://doi.org/10.12989/acc.2022.14.2.079

Effect of shape and amount of transverse reinforcement on lateral confinement of normal-strength concrete columns

Hyeong-Gook Kim [a] and Kil-Hee Kim*

Department of Architectural & Urban System Engineering, Kongju National University, Cheonan 31080, Korea

(*Received January 14, 2022, Revised August 4, 2022, Accepted August 5, 2022*)

Abstract. The amount and configuration of transverse reinforcement are known as critical parameters that significantly affect the lateral confinement of concrete, the ductility capacity, and the plastic hinge length of RC columns. Based on test results, this study investigated the effect of the three variables on structural indexes such as neutral axis depth, lateral expansion of concrete, and ductility capacity. Five reinforced concrete column specimens were tested under cyclic flexure and shear while simultaneously subjected to a constant axial load. The columns were reinforced by two types of reinforcing steel: rectangular hoops and spiral type reinforcing bars. The variables in the test program were the shape, diameter, and yield strength of transverse reinforcement. The interactive influence of the amount of transverse reinforcement on the structural indexes was evaluated. Test results showed that when amounts of transverse reinforcement were similar, and yield strength of transverse reinforcement was 600 MPa or less, the neutral axis depth of a column with spiral type reinforcing bars was reduced by 28% compared with that of a column reinforced by existing rectangular hoops at peak strength. While the diagonal elements of spiral-type reinforcing bars significantly contributed to the lateral confinement of concrete, the strain of diagonal elements decreased with increases of their yield strength. It was confirmed that shapes of transverse reinforcement significantly affected the lateral confinement of concrete adjacent to plastic hinges. Transverse reinforcement with a yield strength exceeding 600 MPa, however, increased the neutral axis depth of normal-strength concrete columns at peak strength, resulting in reductions in ductility and energy dissipation capacity.

Keywords: lateral confinement; neutral axis depth; plastic hinge; spiral; transverse reinforcement

1. Introduction

It is desirous to design reinforced concrete structures (hereinafter, RC) to avoid collapse or critical damage under extreme conditions. However, it is uneconomical to design RC structures to behave within the elastic range against the inertial force caused by earthquakes (Shamin and Shafik 1993). Current seismic design codes, therefore, allow RC structures to be designed to undergo inelastic deformation during seismic events. A column in an RC structure is a critical structural component that supports beams and slabs and transmits load to the foundation; thus, column design should guarantee ductile behavior of columns against seismic loads.

Core concrete in an RC column subjected to axial compression load and flexural moment expands laterally after the spalling of cover concrete. Transverse reinforcement in an RC column constrains the buckling of longitudinal rebars and the lateral expansion of core concrete. Thus, adequate lateral restraints in concrete cores can increase the strength and ductility of RC columns. It is well known that spiral reinforcement has a better lateral confinement effect on concrete than hoop reinforcement, making it advantageous for improving ductility of columns. However, due to difficulties in construction, spiral reinforcement is used less frequently than hoop reinforcement. In addition, placing a large number of internal sub-ties is more effective in terms of the ductility improvement of the column than narrowing the transverse reinforcement because sub-ties increase the core concrete's confinement area and effectively prevent buckling of internal longitudinal rebars (Marinez *et al*. 1984, Moehle and Cavanagh 1985, Mander *et al*. 1988, Yong *et al*. 1989, Muguruma and Watanabe 1990, Muguruma *et al*. 1991, Razvi 1992, Sheikh and Toklucu 1993, Cusson and Paultre 1994, Razvi and Saatcioglu 1999).

Recently, various types of external strengthening methods to improve the lateral deflection and the compressive strength of RC columns have been proposed. Existing experimental studies on externally confined RC members (Ding *et al*. 2019, Moretti 2019, Wang *et al*. 2019, Raoof *et al*. 2020, Zhang *et al*. 2020, Elsamak and Fayed 2021) showed that steel tubes, FRP jackets, aluminum plates and CFRP sheets are effective in confining concrete and reducing the length of plastic hinge, resulting in improving ductility and energy dissipation capacity of the RC members. However, it is important to predict the flexural strength of a pure column without external confinement at the design stage. Over-reinforcement of RC columns may cause brittle fracture due to concrete crushing

*Corresponding author, Professor,
E-mail: kimkh@kongju.ac.kr
[a] Research Assistant Professor,
E-mail: anthk1333@kongju.ac.kr

ISSN: 2287-5301 (Print), 2287-531X (Online)

before longitudinal reinforcements reach the yield strength.

The ACI-318 code (2019) suggests using sub-ties with 135-degree and 90-degree hooks to prevent buckling of longitudinal rebars. However, conventional sub-ties may result in poor filling of concrete due to overcrowding of reinforcement, and deterioration of constructability. For example, the loosening of 90-degree hooks causes a decrease in effective lateral confinement for concrete and buckling of inner longitudinal rebars, which result in abrupt decreases in strength and ductility of the column. For this reason, many existing studies have experimentally and analytically examined the effects of the axial load ratio, shape, and volumetric ratio of transverse reinforcement on the lateral confinement of concrete and the ductility of RC columns. Based on the ACI code, Sheikh and Shafik (1997) proposed a modified equation for determining the amount of transverse reinforcement considering the effect of the shape of the transverse reinforcement and the axial load ratio. They reported that column ductility is affected by the axial load ratio and confinement degree of longitudinal rebars; and, when the axial load ratio is high, at least three internal longitudinal rebars should be constrained to secure the sufficient ductility of the column.

Shin *et al*. (2010) conducted an experimental study on the flexural performance of RC columns with ultrahigh-strength concrete. They adopted the axial compression ratio, the shape of transverse reinforcement, and the transverse reinforcement volumetric ratio as experimental variables. Through regression analysis of experimental results, they proposed a volumetric ratio of transverse reinforcement to make ultrahigh-strength reinforcement concrete columns subjected to an axial load below 40% or more than 40% of the sectional strength have a ductility higher than 4. In addition, for a more rational design of RC columns, they suggested that the shape of the transverse reinforcement and distribution of the longitudinal rebars should be considered in addition to the axial load ratio in calculating the volumetric ratio of the transverse reinforcement.

Yi *et al*. (2012) investigated the effect of axial load ratio, loading path, and location of transverse reinforcement on the confining stress distribution of RC columns; they also used a flexural test to look at the length of plastic hinges for circular RC columns without cover concrete. They found that in an RC column subjected to reversed cyclic loading, the transverse reinforcement provided confinement stress on both the tension and compression sides in the section before concrete crushing; they also found that the maximum lateral strain of the transverse reinforcement in the plastic hinge region was independent of the section location.

Pam and Ho (2011) mentioned that an RC column designed according to the existing design codes that ignored lateral confinement by transverse reinforcement could suffer shear failure due to the increase in flexural strength. Based on existing experimental data for square columns subjected to axial load and bending moment, they proposed a flexural strength enhancement factor considering lateral confinement by transverse reinforcement. They analytically demonstrated that the flexural strength of RC columns, obtained from standard flexural analysis, increased as much as 1.4 times due to the lateral confinement of hoops. By applying the proposed flexural strength enhancement factor, it was possible to predict the flexural strength of laterally confined RC columns with high enough accuracy to be utilized in the practical design.

Shanan *et al*. (2019) experimentally and analytically investigated the effects of the volumetric ratio, spacing, and yield strength of transverse reinforcement on concrete confinement in normal and high-strength concrete columns. They found that the number of sub-ties in the existing rectangular hoops significantly affects the strength and ductility of normal and high-strength concrete columns. The experimental results showed that transverse reinforcement with a yield strength exceeding 500 MPa decreased the ultimate compressive strain of concrete in RC columns.

In many existing studies (Shin *et al*. 2010, Domenico *et al*. 2019, Shanan *et al*. 2019, Chitra and Rugmini 2021, Jing and Huang 2019, Wang *et al*. 2020, Yang *et al*. 2021, Zakerinejad and Soltani 2021, Bai and Li 2021, Halim *et al*. 2021), it was reported that the performance of RC columns depends on the configuration and amount of transverse reinforcement and spiral reinforcement is the most effective in the confinement of concrete. However, the interactive influence of the volumetric ratio and yield strength of transverse reinforcement on the confined concrete under flexural moment remains unclear. In general, the yield strength of the transverse reinforcement is limited to 500-600 MPa in design codes. This limitation is intended to secure the ductile behavior of the structural members by inducing yielding of the transverse reinforcement before concrete crushing and the usability of the structural members by preventing the expansion of diagonal crack width due to increases in rebar spacing. This study evaluated the effects of shape, diameter, and yield strength of transverse reinforcement on lateral confinement of concrete and length of plastic hinges formed at both ends of flexure-dominated RC columns. Moreover, the lateral confinement effects of existing rectangular hoop and the spiral-type transverse reinforcing bars were assessed through the evaluation of the neutral axis depth, the strain distribution of reinforcing steels, the ductility capacity, and the damage degree of the columns.

2. Description of K-type transverse reinforcing bar

As shown in Figs. 1(a) and (b), spiral-type transverse reinforcing bars (hereafter called the K-type transverse reinforcement) are composed of continuous rectangular-shaped hoops and octagonal-shaped sub-ties. K-type transverse reinforcement is made in one piece, so there is no problem loosening the sub-ties due to the buckling of longitudinal rebars. Furthermore, this structure has the advantage of more than halving the time required for reinforcement compared to the existing hoop method. Kim *et al*. (2020) confirmed that when amounts of transverse reinforcement ($\rho_w f_{wy}$) were similar, columns made of K-type transverse reinforcement in grade 500 MPa had flexural strength and ductility more than equivalent to those of columns using conventional rectangular transverse

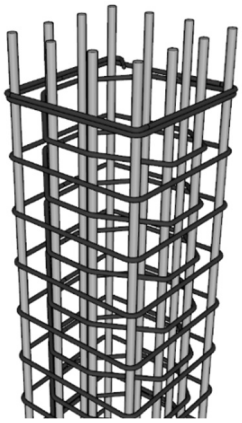

(a) 3D view

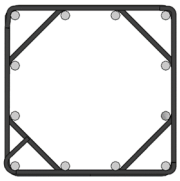

(b) Cross section

(c) Steel surface processing

Fig. 1 Rectangular and octagon-shaped spiral (K-type transverse reinforcing bar)

Table 1 List of specimens

Specimens		Sectional properties				Transverse reinforcement				
		b (mm)	h (mm)	a/d (-)	d (-)	A_w (mm^2)	s (mm)	ρ_w (-)	$f_{wy}{}^*$ (MPa)	$\rho_w f_{wy}{}^*$ (-)
1	H-F5-10	400	400	3.11	D10	71.3	150	0.00475	500	2.38
2	K-F6-10				Ø10	71.3	150	0.00405	600	2.43
3	K-F7-9				Ø9.2	59.4	150	0.00338	700	2.37
4	K-F8-8				Ø8.2	50.2	150	0.00286	800	2.29
5	K-F10-8				Ø8.2	50.2	150	0.00286	1000	2.86

※H: column with hoops, K: column with K-type transverse reinforcement, b: width, h: height, a/d: shear span-to-depth ratio, d: diameter of transverse reinforcement, s: spacing of transverse reinforcement, ρ_w: transverse reinforcement ratio, $f_{wy}{}^*$: yield strength of transverse reinforcement at the design stage

reinforcement. Furthermore, increases in yield strength helped increase flexural strength and ductility when transverse reinforcement ratios were the same.

3. Experimental program

3.1 Description of specimens

A total of four specimens were prepared to evaluate the effects of shape, diameter, and yield strength of transverse reinforcement on lateral confinement and flexural behavior of normal- strength concrete columns. Table 1 presents a list of specimens, while Fig. 2 shows specimen details and locations of strain gauges. H and K in the specimen labels in Table 1 indicate specimens reinforced by existing hoop and K-type transverse reinforcement, respectively. F5, F6, F7, F8, and F10 refer to the grades of transverse reinforcement (for example, F5 = 500 MPa), and numbers 8, 9, and 10 are diameters of transverse reinforcing bars. All specimens had width (b) of 400 mm, height (h) of 400 mm, and length (l) of 2100 mm, and shear span-to-depth ratio (a/d) of 3.11.

Twelve D19 deformed bars of grade SD400 were used as longitudinal rebars for all specimens. The spacing of transverse reinforcement was set to 150 mm. For specimen H-F5-10, 135° and 90° standard hooks were distributed in the width and height directions of the section. In the design stage, $\rho_w f_{wy}$ of all specimens was set in a similar range of 2.38-2.86. When calculating the transverse reinforcement ratio (ρ_w=$A_{sh}/(bs)$), the effective sectional areas of the transverse reinforcement (A_{sh}) of the reference specimen H-F5-10 and the K series specimens were obtained by multiplying the cross-sectional area of the transverse reinforcement (A_w) by 4.0 and 3.41, respectively (Park and Pauley 1975). In this study, specimens to which K-type transverse reinforcement with a yield strength of 500 MPa was applied were excluded from the experimental program by referring to the experimental results of Kim *et al*. (2020).

3.2 Materials

Material properties of concrete and reinforcement are presented in Tables 2 and 3. The design strength of the concrete was 30 MPa, and the maximum diameter of coarse aggregate was 25 mm. For the transverse reinforcement of H-F5-10, D10 deformed bars of grade SD500 were used. The transverse reinforcement of the K series specimens has a different yield strength, and surface-treated steel with diameters from 8.2 to 10 mm was used, as shown in Fig.

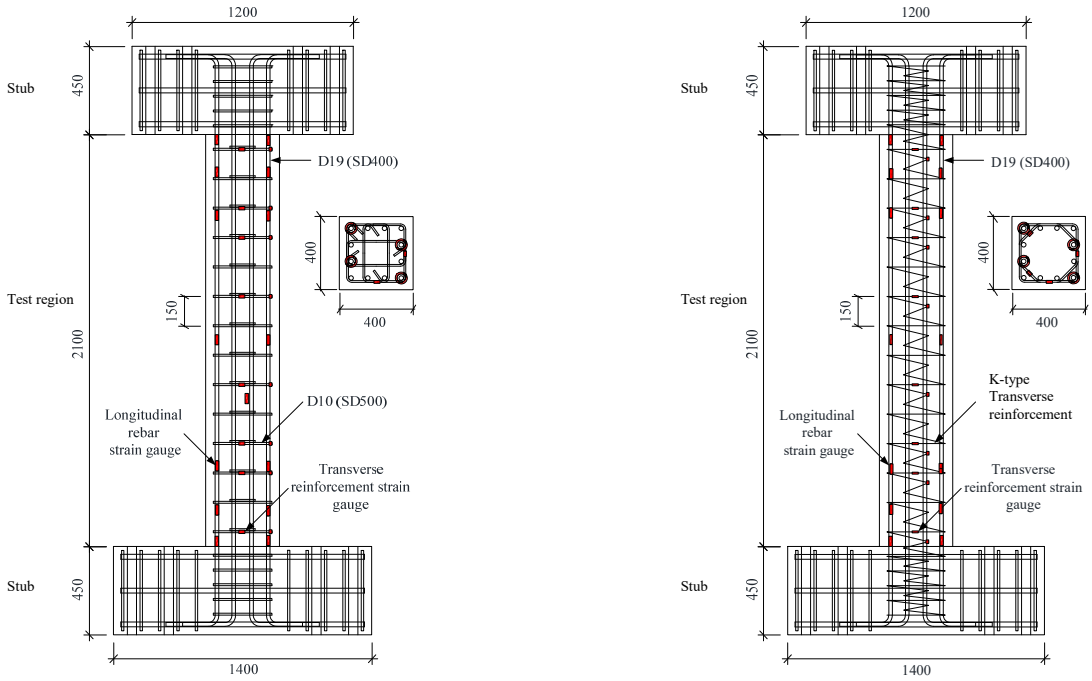

(a) H-F5-10 (b) K series specimens

Fig. 2 Details of specimens (unit: mm)

Table 2 Material properties of concrete

Curing period (days)	G_{max} (mm)	f_{ck} (MPa)	f_{cu} (MPa)	E_c (MPa)	ε_{co} (-)	ε_{cu} (-)
28	25	28.7	26.7	18840.4	0.0027	0.0032

※E_c: elastic modulus of concrete, ε_{co}: maximum compressive strain, ε_{cu}: ultimate compressive strain

Table 3 Material properties of reinforcement

Specimens		Type	A (mm^2)	f_y (MPa)	ε_y(-)	E_s (MPa)
Longitudinal reinforcement		D19	286.5	453.9	0.0024	189,112
Transverse reinforcement	H-F5-10	D10	71.3	534.4	0.0030	177.601
	K-F6-10	Ø10	71.3	624.8	0.0043	162,292
	K-F7-9	Ø9.2	64.2	744.2	0.0047	164,680
	K-F8-8	Ø8.2	50.3	855.6	0.0055	152,068
	K-F10-8	Ø8.2	50.3	1162.3	0.0081	140,916

※A: cross sectional area, f_y: yield strength, ε_y: yield strain, E_s: elastic modulus of reinforcement

1(c). Except for K-F10-8, $\rho_w f_{wy}$ values of specimens, calculated from the actual yield strengths of the steel obtained through tensile test, were in the range of 2.45-2.54, similar to the values set during the experimental plan.

3.3 Loading and measurement plans

Fig. 3 shows a schematic of the loading devices and test setup installed for the quasi-static cyclic loading test of the column specimen. Horizontal and vertical loads were applied to specimens by 1000-kN-capacity actuators. In specimens, an axial load equivalent to 10% of the axial compressive strength (n_o = 0.1) was introduced. Loadings of two cycles each were applied at 2, 4, and 6 times displacement (Δ_y) at the yield of the longitudinal rebars per specimen in each deformation stage, as with the example of the loading protocol for H-F5-10 shown in Fig. 4. Loading was continued until the applied load dropped below 80% of the maximum load. The displacements and drift ratios were measured with two LVDTs installed on the upper and lower stubs. As shown in Fig. 2, strain gauges were installed to evaluate the strain distribution of the longitudinal rebars and transverse reinforcing bars, the lengths of the plastic hinges, and the lateral confinement of the concrete on the compression sides of the section.

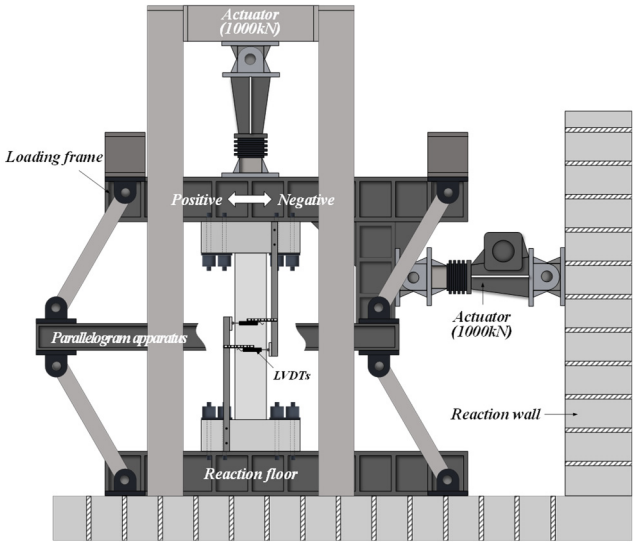

Fig. 3 Schematic of loading devices and test setup

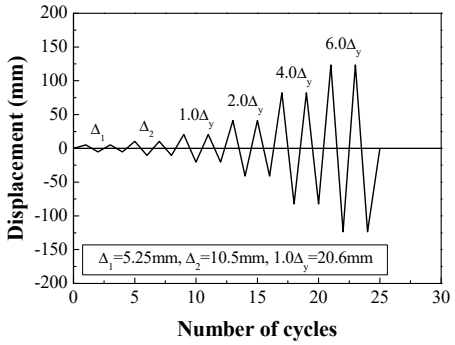

Fig. 4 Example of loading protocol for H-F5-10

4. Experimental results

4.1 Load-diplacement relation

Table 4 summarizes the experimental results for the vital loading stages and corresponding displacement; Fig. 5 shows load-displacement hysteretic curves of the specimens. In all specimens, the first flexural cracks developed at the drift ratio of 0.25%, equivalent to a displacement (Δ) of 5.25 mm. For specimens other than K-F6-10, longitudinal rebars reached their yield strength at a drift ratio of 0.72-0.99%. The yield displacement (Δ_y) of K-F6-10 was 15.1 mm, which was the smallest value among all specimens. Yielding of the transverse reinforcement in the flexure-dominated column specimens did not appear until the experiment was terminated. The average absolute values of the maximum strength (P_{max}) in the positive and negative loading directions were in a range of 275.8-285.4 kN, and ultimate load (P_u) values were also similar regardless of the shapes of the transverse reinforcement. As the displacement increased after P_{max}, the strengths of all specimens gradually decreased due to spalling and crushing of concrete at both ends.

For specimen H-F5-10, the applied load dropped below P_u at an average displacement equivalent to about $4.7\Delta_y$, and the K series specimens reached P_u at an average displacement equivalent to or greater than $5\Delta_y$. The average displacement of K-F6-10 at P_u was 98.3 mm, which was the smallest value among all specimens. However, this value was equivalent to 6.5 times the yield displacement, showing that K-F6-10 had the largest deformation capacity among all specimens. The load-displacement relation of specimens showed that though the shape of the transverse reinforcement had a slight effect on the maximum strength of the columns, it significantly affected their deformation capacity. In addition, for specimens with similar value of

Table 4 Results of cyclic loading tests

Specimens			Loading direction	At yielding of reinforcement		At peak load		At 80% of peak load		Failure mode
No.	Name	$\rho_w f_{wy}$ (-)		P_y (kN)	Δ_y (mm)	P_{max} (kN)	Δ_{max} (mm)	P_u (kN)	Δ_u (mm)	
1	H-F5-10	2.54	Positive	257.4	20.6	286.4	39.5	229.1	109.6	Flexural
			Negative			-284.3	-38.0	-227.4	-82.9	
2	K-F6-10	2.53	Positive	233.6	15.1	276.5	29.8	221.2	94.7	Flexural
			Negative			-275.1	-35.7	-220.1	-101.9	
3	K-F7-9	2.52	Positive	-261.4	-19.9	278.8	35.7	222.8	106.1	Flexural
			Negative			-291.1	-39.5	-232.8	-103.5	
4	K-F8-8	2.45	Positive	253.7	20.8	280.6	32.3	224.5	108.4	Flexural
			Negative			-278.6	-32.9	-222.9	-106.3	
5	K-F10-8	3.32	Positive	250.7	19.9	283.1	39.5	226.5	104.6	Flexural
			Negative			-282.9	-39.1	-226.3	-97.4	

※f_{wy}: yield strength of transverse reinforcement measured from tensile test, P_y: yield load, P_{max}: maximum load, P_u: ultimate load (= $0.8P_{max}$), Δ_y: yield displacement, Δ_{max}: displacement at P_{max} and Δ_u: ultimate displacement

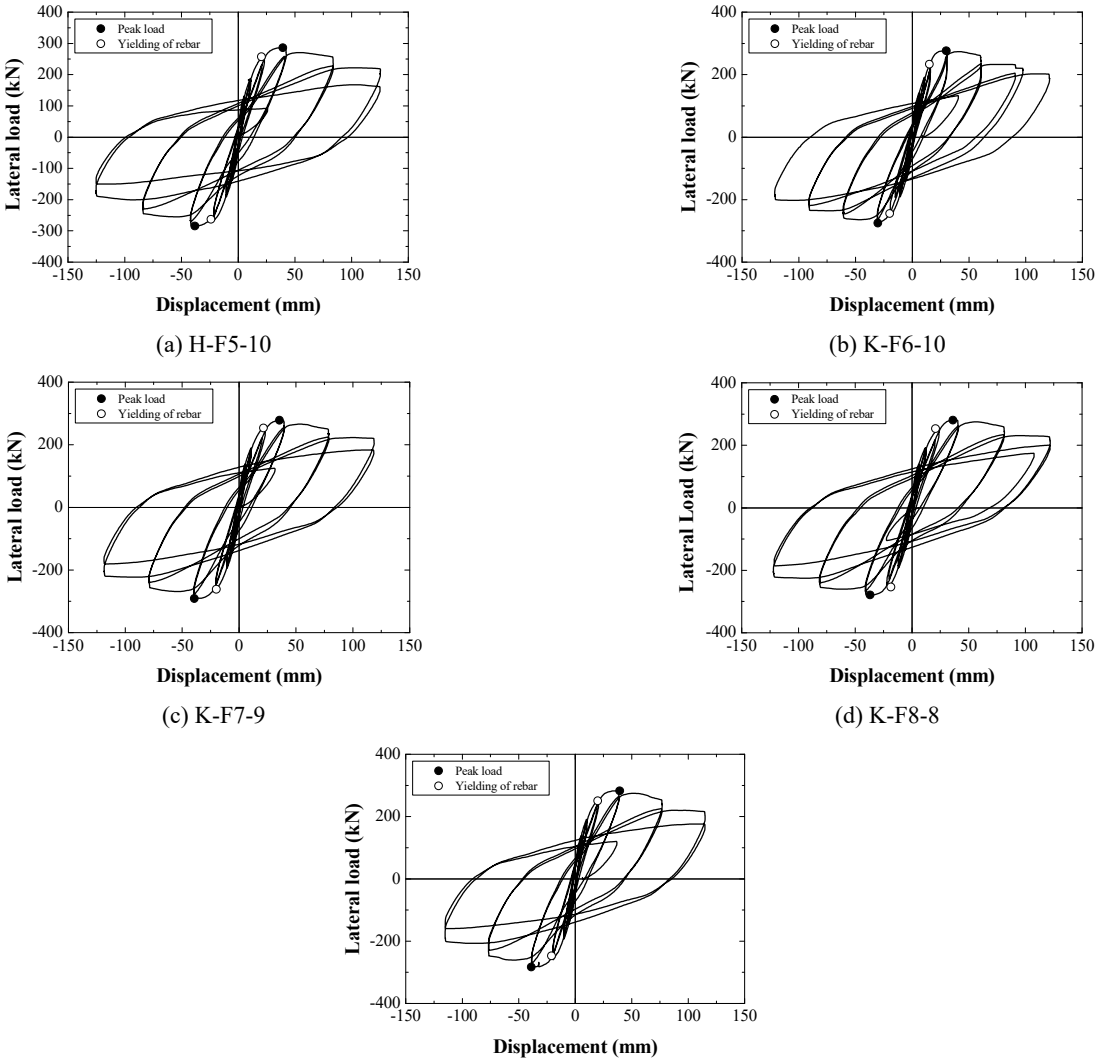

(a) H-F5-10

(b) K-F6-10

(c) K-F7-9

(d) K-F8-8

(e) K-F10-8

Fig. 5 Lateral load-displacement relations

$\rho_w f_{wy}$, the deformation capacity of the specimen decreased as the transverse reinforcement ratio (ρ_w) was reduced. This was because, compared to existing hoops, K-type transverse reinforcement effectively constrained core concrete in the plastic hinge region, delaying crushing and preventing buckling of longitudinal rebars. This result can be confirmed through the crack patterns of specimens and the strain distributions in reinforcement.

4.2 Failure modes

Fig. 6 shows crack patterns of specimens at failure. In all specimens, initial flexural cracks occurred at both ends at a drift ratio of 0.25%. New flexural cracks facing centers of specimens and flexure-shear cracks connected with them occurred at drift ratio of 0.5%. For H-F5-10, spalling of cover concrete occurred at both ends at a displacement equivalent to $2\Delta_y$, and concrete crushing occurred at a displacement equivalent to $4\Delta_y$. In addition, buckling of the corner and inner longitudinal rebars, as well as loosening of a 90º hook, was observed at both ends.

For K-6F-10, whereas the pattern and distribution of cracks were similar to those in the reference specimen, the crushing of concrete occurred at both ends at a displacement equivalent to $6\Delta_y$. Spalling of cover concrete in K-F7-9, K-F8-8, and K-F10-8 occurred at a displacement equivalent to $4\Delta_y$. Crushing of concrete appeared at a displacement equivalent to about $5\Delta_y$. No buckling of longitudinal rebars was found in any of the K series specimens. The delay of concrete crushing and no buckling of longitudinal rebars in the K series specimen show that, compared to the existing hoops, the continual octagon steel in the K-type transverse reinforcement effectively constrained the core concrete and longitudinal rebars.

4.3 Strain distribution

4.3.1 Strain distribution in longitudinal rebar

Fig. 7 shows the strain distribution in the longitudinal rebar for the specified positive and negative displacement levels. After the yielding of the longitudinal rebar, the strain of the tension side longitudinal rebars of the K series

(a) H-F5-10 (b) K-F6-10 (c) K-F7-9 (d) K-F8-8 (e) K-F10-8

Fig. 6 Crack patterns in specimens at failure

specimens rapidly increased. Meanwhile, the increase in the strain of the tension side longitudinal rebars of the reference specimen slowed or decreased. The plastic hinge length for each specimen is the distance from the location where, after maximum strength, the strain of the longitudinal rebar reached the yield strain until the upper or lower stub of the column, as shown in Fig. 7. The plastic hinge of H-F5-10 was about 600 mm at Δ_y, and 704 mm at $2\Delta_y$, an increase of 17%. The length of the plastic hinge of the K series specimen was about 420 mm at Δ_y, which was 1.24 times the effective depth (d = 338 mm). After that, despite the increase in displacement, the length of the plastic hinge did not increase significantly. It was found that when $\rho_w f_{wy}$ values of columns are similar, the shape of transverse reinforcement has a significant effect on the length of the plastic hinge.

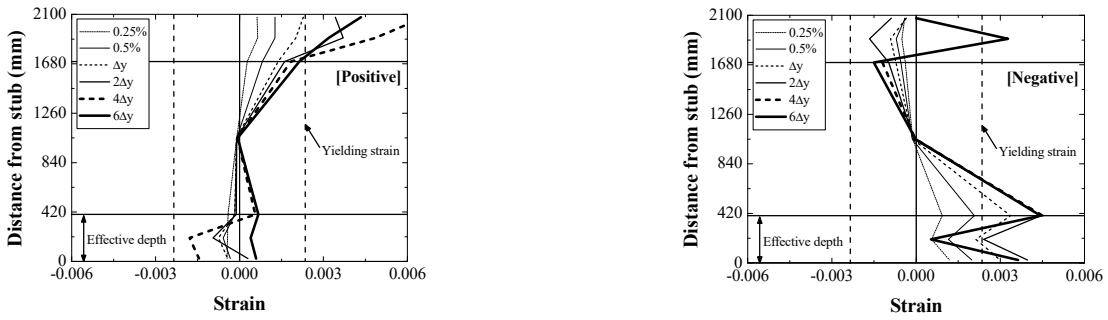

(a) H-F5-10

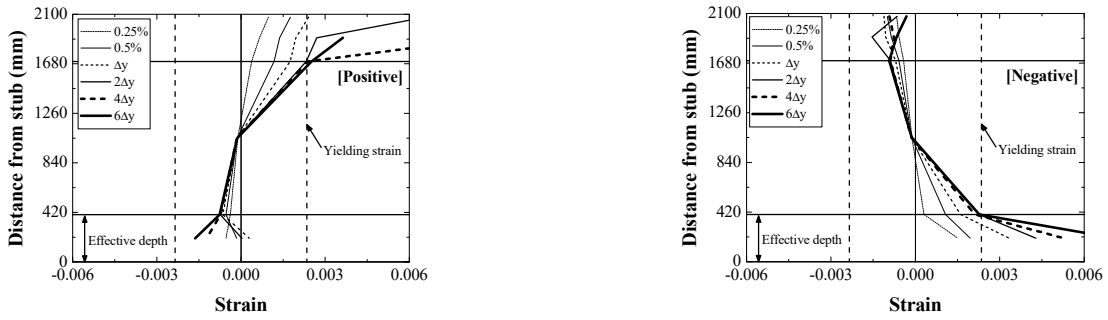

(b) K-F6-10

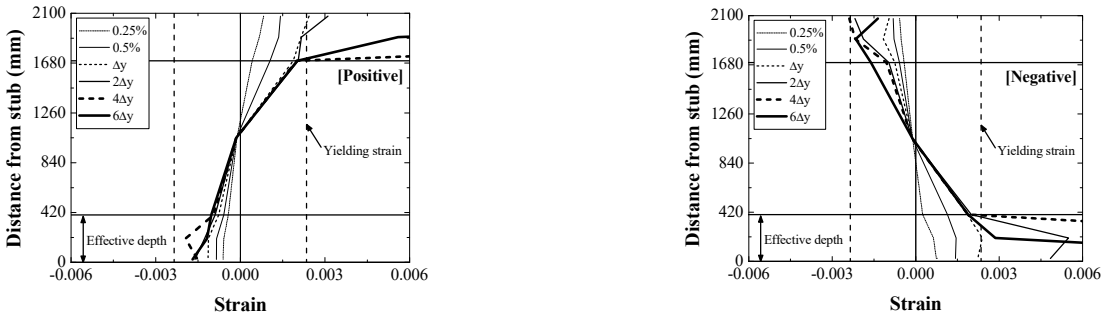

(c) K-F7-9

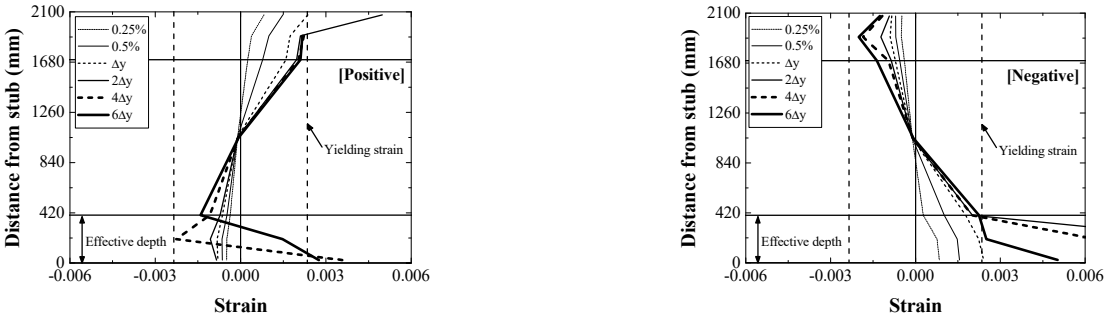

(d) K-F8-8

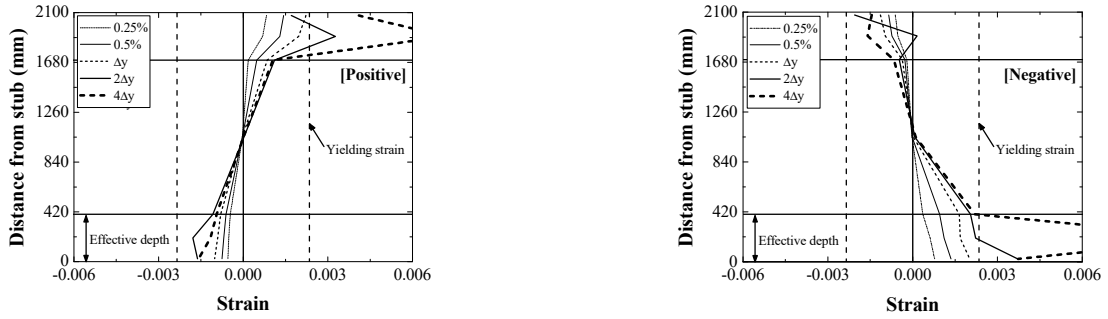

(e) K-F10-8

Fig. 7 Strain distribution in longitudinal rebars

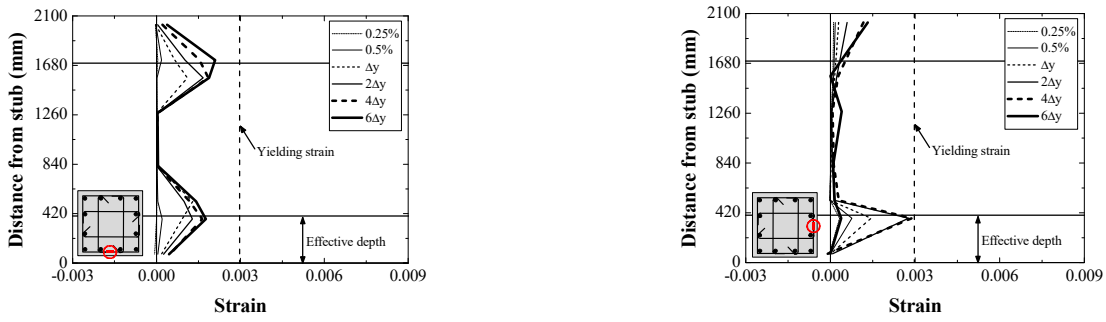

(a) H-F5-10

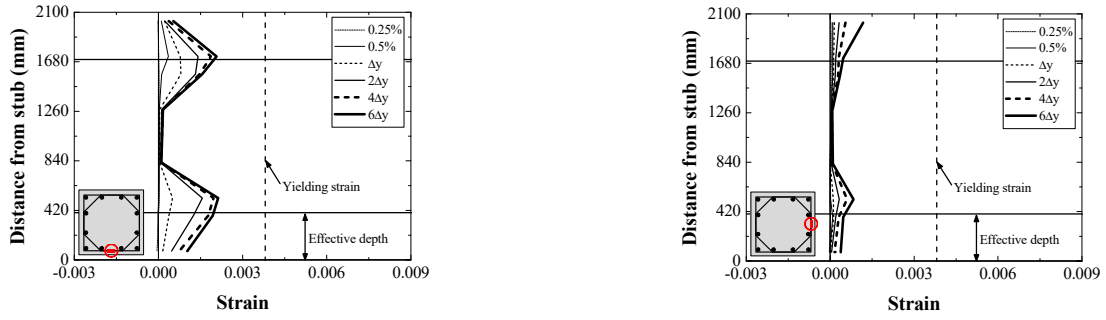

(b) K-F6-10

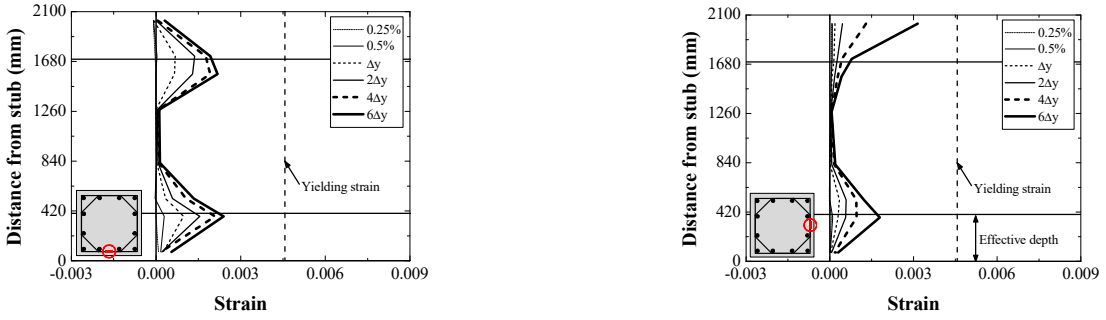

(c) K-F7-9

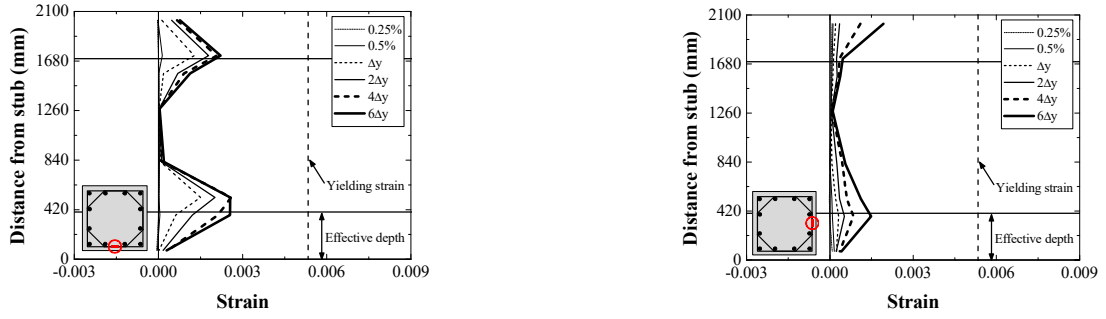

(d) K-F8-8

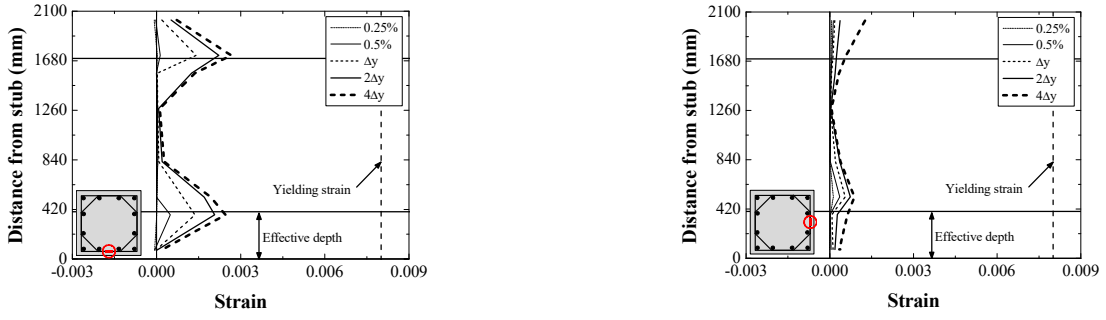

(e) K-F10-8

Fig. 8 Strain distributions of vertical and horizontal elements in transverse reinforcement

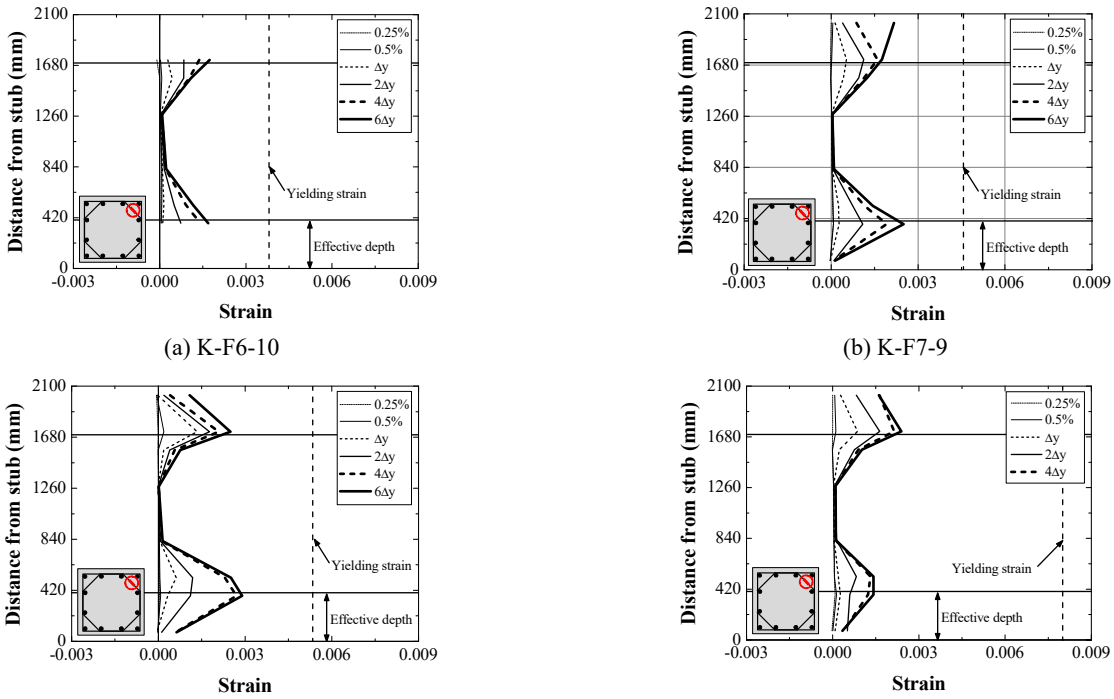

(a) K-F6-10 (b) K-F7-9

(c) K-F8-8 (d) K-F10-8

Fig. 9 Strain distributions of diagonal element in K-type transverse reinforcement

4.3.2 Strain distribution in transverse reinforcement

Fig. 8 presents the strain distribution of vertical and horizonal elements in the transverse reinforcement for the specified positive displacement levels. In the case of the reference specimen, they exhibited a strain distribution of transverse reinforcements placed in the loading direction (the bottom side of the cross-section) and perpendicular to the loading direction (the right side of the cross-section). Fig. 9 presents strain distributions of transverse reinforcements placed in diagonal direction for K series specimens.

All specimens showed highest strains in transverse reinforcements located as far as the effective depth (d) from both ends. In the reference specimen, the maximum strain of the transverse reinforcement placed in the loading direction was 0.00164, which corresponds to about 55% of the yield strain (ε_y = 0.003). Meanwhile, the maximum strain of the transverse reinforcement placed perpendicular to the loading direction reached the yield strain. This indicates that the transverse reinforcement placed perpendicular to the loading direction could not sufficiently resist the buckling of longitudinal rebars and the lateral expansion of concrete subjected to the axial load flexural moment. In the case of the K series specimens, the strain of the transverse reinforcement placed in all directions did not reach the yield strain until failure, implying that it had a sufficient resistance to shear force, axial compression load, and flexural moment. Furthermore, the strain of the octagon-shaped reinforcement placed in the diagonal direction was higher than that of the transverse reinforcement placed in other directions. This shows that the octagon-shaped sub-ties contributed significantly to resisting the applied shear force and the lateral expansion of core concrete.

5. Discussion and analysis

5.1 Neutral axis depth ratio

The volumetric ratio and shape of transverse reinforcement affect the flexural strength of RC columns. This section demonstrates the effect of each variable employed in this study on the neutral axis depth (c) of square columns based on experimental results. Fig. 10 compares the neutral axis depth formed on the cross-section below the top stubs of specimens. The X and Y axes in the figure present the names of specimens and the neutral axis depth ratios (c/d), respectively. The strain distribution of the internal longitudinal rebars was assumed to be linear until the displacement reached $2\Delta_y$. The distance from the compression edge to the neutral axis was estimated using the strains of tensile and compressive-side longitudinal rebars and the cross-sectional properties of specimens.

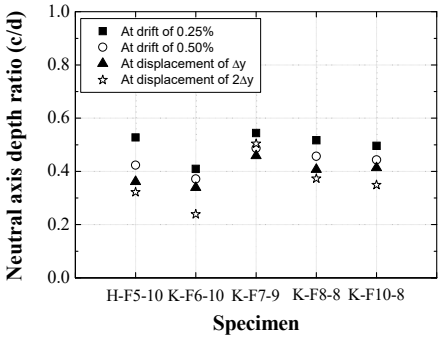

Fig. 10 Neutral axis depth ratio of specimens at specified displacement levels

5.1.1 Effect of shape of transverse reinforcement (H-F5-10 vs. K-F6-10)

The neutral axis depth ratios of H-F5-10 and K-F6-10 showed a decreasing trend as displacement increased. Except for when the displacement was equivalent to Δ_y, the neutral axis depth ratios of K-F6-10 were lower than those of H-F5-10. Meanwhile, the decrement of c/d was higher in H-F5-10 until Δ_y than K-F6-10. While c/d of K-F6-10 was about 28% smaller than that of H-F5-10, the strength of H-F5-10 at $2\Delta_y$ was about 4% higher than that of K-F6-10. This indicates that when $\rho_w f_{wy}$ was similar and the yield strength was 600 MPa or less, concrete on the compression side with a relatively small area constrained by K-type transverse reinforcement could resist the same level of flexural moment.

5.1.2 Effect of amount of transverse reinforcement (K series specimens)

The average maximum strength (P_{max}) of K-F6-10 and K-F7-9, having the same shape and values of $\rho_w f_{wy}$, were similar (see Table 4); however, c/d of K-F7-9 at maximum strength was more than two times higher than that of K-F6-10. Moreover, c/d of K series specimens other than K-F6-10 after a drift ratio of 0.25% was larger than those of the reference specimens. This indicates that even if the K-type transverse reinforcement had a shape that was effective for lateral confinement of concrete compared to existing hoops, lateral confinement for concrete decreased when amount of transverse reinforcement decreased to lower than a specific amount. Moreover, the lateral confinement effect depended on the transverse reinforcement ratio rather than on the yield strength of the transverse reinforcement. It can be seen that the minimum transverse reinforcement ratio (ρ_w) required for lateral confinement of the column specimens used in this study was about 0.00338. According to the research results of JICE (1990), when the compression strength of concrete was less than 50 MPa and the volumetric ratio of the spiral reinforcement was less than 1%, the lateral confinement effect was significantly affected by the compressive strength of concrete, rather than by the yield strength of the spiral reinforcement. Therefore, in the case of increasing the yield strength instead of reducing the amount of confining steel in the K-type transverse reinforcement, the concrete should also have a high compressive strength if lateral confinement effect by K-type transverse reinforcement is to be expected.

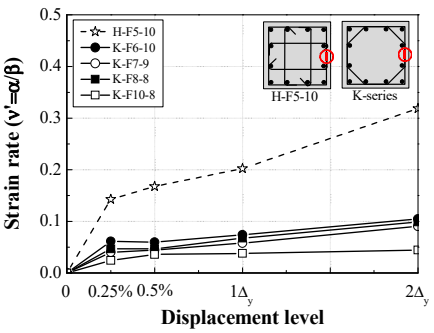

Fig. 11 Strain rate between concrete and transverse reinforcement

5.2 Strain rate

Strains of the concrete on the compression side in the plastic hinge regions and the transverse reinforcements were compared to investigate the effects of the design parameters on the lateral confinement of concrete with the increase in displacement. Fig. 11 compares the strain rate ($v' = \alpha/\gamma$) for the specified displacement levels. α is the ratio of the measured strain (ε_{wi}) to the yield strain (ε_{wy}) of the transverse reinforcements and γ is the ratio of the compressive strain of concrete (ε_{ci}) to the strain of concrete at peak compressive stress (ε_{co}). ε_{ci} was estimated via linear analysis of the strain distribution of longitudinal rebars, as shown in Fig. 9. The strain of the transverse reinforcement placed perpendicular to the loading direction, in Fig. 8, was employed as ε_{wi}.

v' of the reference specimen H-F5-10 at 0.25% drift ratio was 0.14, at least 2.3 times higher than that of the K series specimens. v' of H-F5-10 increased almost linearly until $2\Delta_y$, and v' at that point was about 0.32. v' of the K series specimens at 0.25% drift ratio was in the range of 0.02-0.06. Unlike the reference specimen, v' of the K series specimens was found to be less than 0.1 until $2\Delta_y$. Furthermore, v' of K-F10-8 was the lowest among the K series specimens. However, it should be noted that the diagonal elements of the octagon-shaped sub-ties in the K-type transverse reinforcement significantly contributed to the lateral confinement of the concrete in the plastic hinge regions. In addition, α for the diagonal elements decreased with increase of yield strength of the transverse reinforcement, as shown in Fig. 8. This clearly showed that the shape of transverse reinforcement significantly affected the lateral confinement of concrete.

5.3 Ductility capacity

In this section, the ductility capacity of column specimens for reversed cyclic loading was evaluated through the displacement ductility ratio ($\mu = \Delta_u/\Delta_y$). μ for flexural-dominated columns can be defined as the ratio of maximum displacement (Δ_u) to yield displacement (Δ_y). Fig. 12 shows a comparison of μ for each specimen. Δ_y and Δ_u of H-F5-10, shown in Table 4, were 20.6 mm and

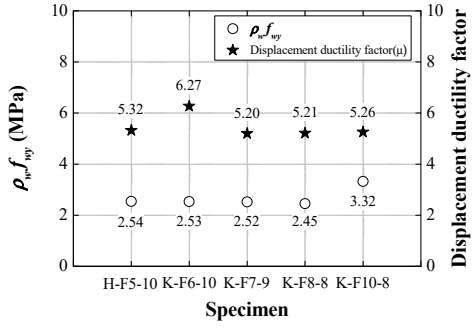

Fig. 12 Displacement ductility

109.6 mm, respectively; μ of this specimen was 5.32. μ of K-F6-10, calculated with the same method, was 6.27, an approximately 1.18 times increase compared to the reference specimen. This shows that when f_{wy} is less than 600 MPa and $\rho_w f_{wy}$ is 2.53 or more, the K-type transverse reinforcement can effectively improve the ductility capacity of RC columns compared to the existing hoops. On the other hand, other specimens in the K series showed an average of 1.8% lower ductility capacity compared to the reference specimen. μ of K-F10-8 increased by 1.1% compared with that of K-F7-9. It can be seen that the effect of the shape and amount of transverse reinforcement on the ductility capacity of the columns, shown in Fig. 11, had an opposite trend to the neutral axis depth ratio shown in Fig. 9. This shows that, when the transverse reinforcement ratio is reduced below a certain level, increasing the yield strength of transverse reinforcement has no influence on the ductility capacity of normal-strength concrete columns.

In Figs. 8 to 11, it can be inferred that the stress of concrete on the compression side of the K series specimens, except for K-F6-10, reached the ultimate compressive strength early, before the strain of the longitudinal rebars reached $2\Delta_y$. This would eventually lead to decreases in ductility capacity of K-F7-9, K-F8-8, and K-F10-8. Differences in shape, diameter, and yield strength of transverse reinforcement significantly affected the neutral axis depth, the lateral confinement of concrete, and the ductility capacity of RC columns. However, it should be noted that even though the shape of K-type transverse reinforcement is more effective for the lateral confinement of concrete, a decrease in the diameter or an increase in the yield strength of transverse reinforcement reduces the lateral confinement effect of a normal-strength concrete column, resulting in a decrease in ductility capacity.

5.4 Energy dissipation and damage assessment

5.4.1 Energy dissipation

Table 5 shows a comparison of the cumulative hysteretic energy dissipation (ΣHE_i) of each specimen up to the specified displacement. ΣHE at a given cycle is calculated as the summation of the hysteretic energies dissipated during the specified and preceding cycles. HE can be determined from the area enclosed by the hysteretic loop at each cycle.

ΣHE_i values of the K series specimens up to the displacement of 10.5 mm were more than double that of the reference specimen. This was because, even under a displacement smaller than Δ_y, the K-type transverse reinforcement effectively constrained the core concrete so that the initial strength increased. On the other hand, among ΣHE_i values of specimens up to the displacement equivalent to $4\Delta_y$, the highest value found was for the reference specimen, while K-F6-10, which showed the highest ductility, absorbed minimum strain energy. This was because, when K-F6-10 reached Δ_y, the maximum strength had the lowest values among all specimens, as shown in Table 4. Meanwhile, differences of ΣHE_i between reference specimen and K series specimens at $6\Delta_y$ were lower than 7%, and differences of ΣHE_i between K series specimens were below 3%. This shows that when the amount of transverse reinforcement in K-type transverse reinforcement was lower than a certain amount, the energy dissipation capacity was not significantly affected by the shape or yield strength of the transverse reinforcement.

5.4.2 Damage degree level of RC columns under cyclic loading

Damage to specimens by cyclic loading was examined using load and displacement of specimens observed during the test. The damage index model (DI) and damage degree level proposed by Park and Ang (1985) were used for damage degree assessment. PA damage index was calculated using Eqs. (1) and (2). The five damage degree levels and damage index for reinforced concrete members are presented in Table 6.

$$DI = \frac{\Delta_i}{\Delta_u} + \beta \frac{\Sigma HE_i}{P_y \Delta_u} \quad (1)$$

$$\beta = 0.7^{\rho_s}\left(-0.447 + 0.073\frac{l}{d} + 0.24 n_o + 0.314\rho_t\right) \quad (2)$$

where Δ_i: maximum displacement at each drift ratio; β: a non-negative parameter based on cyclic loading effect; ρ_s: volumetric ratio of confining steel; ρ_t : longitudinal reinforcement ratio as a percentage (= 0.75% if $\rho_t <$ 0.75%); n_o: normalized axial stress (= 0.2 if $n_o < 0.2$); and l/d: shear span ratio (=1.7 if $l/d < 1.7$).

Fig. 13 shows the damage degree of each specimen with respect to the increase in displacement. Overall, as displacement increased, the PA damage index of K-F6-10 was the lowest among specimens, and the PA damage indexes of the remaining specimens were similar. For

Table 5 Cumulative hysteretic energy dissipation

Specimens	ΣHE_i at Δ_i (kN·m)					
	Up to 5.25 mm	Up to 10.5 mm	Up to Δ_y	Up to $2\Delta_y$	Up to $4\Delta_y$	Up to $6\Delta_y$
H-F5-10	1.26	1.62	9.16	31.64	97.34	198.51
K-F6-10	1.34	4.10	8.93	23.46	66.03	188.34
K-F7-9	1.22	3.85	10.88	31.36	92.27	191.44
K-F8-8	1.22	3.92	10.10	27.69	80.57	184.77
K-F10-8	1.47	4.34	11.52	32.68	94.06	192.76

Table 6 Five damage degree levels and damage index for RC members

Damage degree level	Damage Index (DI)	Damage state
Slight	DI < 0.1	No damage or minor cracking
Minor	0.1 < DI < 0.25	Minor damage, light cracking throughout
Moderate	0.25 < DI < 0.4	Extensive large cracks, spalling of concrete cover
Severe	0.4 < DI < 1.0	Extensive crushing of concrete, visible buckling of reinforcement
Collapse	DI > 1.0	Partial or total collapse of RC members

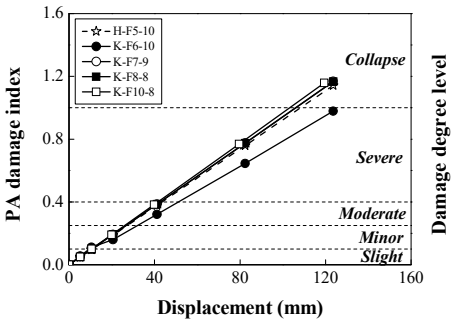

Fig. 13 Damage degree levels based on PA damage index

displacement in the range of 15-20 mm, equivalent to Δ_y, the PA damage indexes of specimens were 0.16-0.19, indicating minor damage. PA damage indexes until displacement in the range of 66-94 mm, equivalent to $4\Delta_y$, were different; however, all specimens had severe damage. Specimens having displacements in the range of 188-123 mm, equivalent to $6\Delta_y$, showed damage at a level of collapse, except for K-F6-10. Figs. 11 and 12 show that when values of $\rho_w f_{wy}$ were similar, H-F5-10, K-F7-9, K-F8-8, and K-F10-8 had similar levels of displacement ductility and damage degree. These structural performance indexes of H-F5-10 were affected by the shape of transverse reinforcement; however, the indexes of K-F7-9, K-F8-8, and K-F10-8 were affected by the amount or diameter of transverse reinforcement. This shows that even when the amount of reinforcing steel used was reduced by 30~40%, the structural performances of columns with K-type transverse reinforcement were similar to that of a column with existing hoops.

6. Conclusions

Based on an experiment using RC column specimens with existing hoop and K-type transverse reinforcement under cyclic loading, the effects of shape, diameter, and yield strength of transverse reinforcement on lateral confinement and ductility capacity of columns were investigated. The experimental results show that K-type transverse reinforcement was more effective for lateral confinement of concrete than existing hoops. For columns with K-type transverse reinforcement, increasing the yield strength of reinforcing steel instead of reducing its diameter resulted in similar performance of RC columns in terms of strength, ductility, and energy dissipation capacity. The diagonal elements of the K-type transverse reinforcement contributed significantly to the lateral confinement of concrete. It was found that the shape and amount of transverse reinforcement, rather than its yield strength, play an important role in increasing the lateral confinement of concrete. However, when applying K-type transverse reinforcement with a yield strength exceeding 600 MPa to a normal-strength concrete column, the stress of concrete on the compression side reaches the ultimate compressive strength early, resulting in a decrease in ductility capacity and in energy dissipation. It is considered that concrete used for columns should have high compressive strength of 50 MPa or more to induce lateral confinement effect by K-type transverse reinforcement having yield strength exceeding 600 MPa. High-strength concrete is being widely used in prestressed concrete members. Recently high-strength concrete is widely used in prestressed concrete members. K-type transverse reinforcement with high constructability is expected to be an alternative for improving the seismic performance of prestressed concrete columns.

Acknowledgments

This research was supported by UNDERGROUND CITY OF THE FUTURE program funded by the Ministry of Science and ICT.

References

ACI Committee (2019), Building Code Requirements for Structural Concrete (ACI 318-19) and Commentary, American Concrete Institute, Farmington Hills, MI, USA.

Bai, J. and Li, S. (2021), "Seismic behavior of prefabricated high-strength concrete columns confined by overlapping stirrups", *Struct. Eng. Mech., Int. J.*, **79**(5), 579-591. https://doi.org/10.12989/sem.2021.79.5.579

Chitra, M. and Rugmini, B.K. (2021), "Performance of reinforced concrete columns confined with spiral reinforcement", *Struct. Des. Tall. Build.*, **30**(10), 1-15. https://doi.org/10.1002/tal.1859

Cusson, D. and Paultre, P. (1994), "High-Strength Concrete Columns Confined by Rectangular Ties", *J. Struct. Eng.*, **120**(3), 783-804. https://doi.org/10.1061/(ASCE)0733-9445(1994)120:3(783)

Ding, F., Yin, Y., Wang, L., Yu, Y., Luo, L. and Yu, Z. (2019), "Confinement coefficient of concrete-filled square stainless steel tubular stub columns", *Steel Compos. Struct., Int. J.*, **30**(4), 337-350. https://doi.org/10.12989/scs.2019.30.4.337

Domenico, D., Falliano, D. and Ricciardi, G. (2019), "Confinement effect of different arrangements of transverse reinforcement on axially loaded concrete columns: An experimental study", *J. Mech. Behav. Mater.*, **28**, 13-19. https://doi.org/10.1515/jmbm-2019-0003

Elsamak, G. and Fayed, S. (2021), "Flexural strength of RC beams using externally bonded aluminum plates: An experimental and numerical study", *Adv. Concr. Constr., Int. J.*, **11**(6), 481-492. https://doi.org/10.12989/acc.2021.11.6.481

Halim, N.H.F.A., Alih, S.C. and Vafaei, M. (2021), "Seismic behavior of RC columns internally confined by CFRP strips", *Adv. Concr. Constr., Int. J.*, **12**(3), 217-225. https://doi.org/10.12989/acc.2021.12.3.217

JICE (1990), High-strength concrete subcommittee report, Japan Institute of construction Engineering, Tokyo, Japan.

Jing, D.H. and Huang, L.B. (2019), "Effect of transverse reinforcement on rectangular concrete columns with MTSTR", *Mag. Concr. Res.*, **71**(2), 1-44. https://doi.org/10.1680/jmacr.17.00380

Kim, H.G., Jeong, C.Y., Kim, D.H. and Kim, K.H. (2020), "Confinement Effect of Reinforced Concrete Columns with Rectangular and Octagon-Shaped Spirals", *Sustainability*, **12**(9), 7981. https://doi.org/10.3390/su12197981

Mander, J.B., Priestley, M.J.N. and Park, R. (1988), "Observed stress-strain behavior of confined concrete", *J. Struct. Eng.*, **114**(8), 1827-1849. https://doi.org/10.1061/(ASCE)0733-9445(1988)114:8(1827)

Marinez, S., Nilson, A.H. and Slate, F.O. (1984), "Spirally reinforced high-strength concrete columns", *ACI Struct. J.*, **81**(5), 431-442.

Moehle, J. and Cavanagh, T. (1985), "Confinement effectiveness of crossties in RC", *J. Struct. Div.*, **111**(10), 2105-2120. https://doi.org/10.1061/(ASCE)0733-9445(1985)111:10(2105)

Moretti, M.L. (2019), "Effectiveness of different confining configurations of FRP Jackets for concrete columns", *Struct. Eng. Mech., Int. J.*, **72**(2), 155-168. https://doi.org/10.12989/sem.2019.72.2.155

Muguruma, H. and Watanabe, F. (1990), "Ductility improvement of high-strength concrete columns with lateral confinement", *ACI Spec. Publ.*, **121**, 47-60. https://doi.org/10.14359/2783

Muguruma, H., Watanabe, F. and Tanaka, H. (1991), "Ductile Behaviour of High-Strength Columns Confined by High-Strength Transverse Reinforcement", *ACI Spec. Publ.*, **128**, 877-891.

Pam, H.J. and Ho, J.C.M. (2011), "Flexural strength enhancement of confined reinforced concrete columns", *Proceedings, Institution of Civil Engineers, Struct. Build.*, **146**(4), 363-370. https://doi.org/10.1680/stbu.2001.146.4.363

Park, Y.J. and Ang, A.H.S. (1985), "Mechanistic seismic damage model for reinforced concrete", *J. Struct. Eng.*, **111**(4), 722-739. https://doi.org/10.1061/(ASCE)0733-9445(1985)111:4(722)

Park, R. and Pauley, T. (1975), *Reinforced Concrete Structures*, John Wiley and Sons, New York, USA.

Raoof, S.M., Ibraheem, O.F. and Tais, A.S. (2020), "Confinement effectiveness of CFRP strengthened concrete cylinders subjected to high temperatures", *Adv. Concr. Constr., Int. J.*, **9**(6), 529-535. https://doi.org/10.12989/acc.2020.9.6.529

Razvi, S.R. (1992), "Strength and ductility of confined concrete", *J. Struct. Eng.*, **118** (6), 1590-1607. https://doi.org/10.1061/(ASCE)0733-9445(1992)118:6(1590)

Razvi, S.R. and Saatcioglu, M. (1999), "Circular high-strength concrete columns under concentric compression", *ACI Struct. J.*, **96**(5), 817-826.

Shamim, A.S. and Shafik, S.K. (1993), "Confined concrete columns with stubs", *ACI Struct. J.*, **90**(4), 414-431.

Shamim, A.S. and Shafik, S.K. (1997), "A performance-based approach for the design of confining steel in tied columns", *ACI Struct. J.*, **94**(4), 421-431.

Shanan, M.A., El-Zanati, A.H., Anis, A.R. and Metwally, K.G. (2019), "Effect of confinement with lateral reinforcement on normal & high strength concrete columns", *Proceedings of the 2019 World congress on Advances in Structural Engineering and Mechanics* (*ASEM'19*), Jeju, Korea, September.

Sheikh, S.A. and Toklucu, M.T. (1993), "Reinforced concrete columns confined by circular spirals and hoops", *ACI Struct. J.*, **90**(5), 542-553.

Shin, S.W., Kim, J.K. and Ahn, J.M. (2010), "Transverse reinforcement of RC columns considering effective lateral confining reduction factor", *J. Asian Archit. Build. Eng.*, **9**(2), 501-508. https://doi.org/10.3130/jaabe.9.501

Wang, J., Yang, J. and Cheng, L. (2019), "Experimental study of seismic behavior of high-strength RC columns strengthened with CFRP subjected to cyclic loading", *J. Struct. Eng.*, **145**(2), 1-14. https://doi.org/10.1061/(ASCE)ST.1943-541X.0002251

Wang, P., Shi, Q., Wang, F. and Wang, Q. (2020), "Seismic behavior of concrete columns with high-strength stirrups", *Earthq. Struct.*, **18**(1), 15-25. https://doi.org/10.12989/eas.2020.18.1.015

Yang, K., Shi, Q.X. and Lin, Q. (2021), "Seismic Performance and Confinement Reinforcement Design of High-Strength Concrete Confined with High-Strength Stirrups", *Adv. Struct. Eng.*, **24**(10), 2061-2075. https://doi.org/10.1177/1369433221992491

Yi, W.J., Li, P. and Kunnath, S.K. (2012), "Experimental Studies on Confinement Effect of Steel Hoops in Concrete", *ACI Struct. J.*, **109**(1), 3-10.

Yong, Y.K., Nour, M.G. and Nawy, E.G. (1989), "Behavior of laterally confined high-strength concrete under axial loads", *J. Struct. Eng.*, **114**(2), 332-351. https://doi.org/10.1061/(ASCE)0733-9445(1988)114:2(332)

Zakerinejad, M. and Soltani, M. (2021), "Compressive behavior of RC members with rectangular continuous transverse reinforcement", *Struct. Concr.*, **22**(6), 3396-3413. https://doi.org/10.1002/suco.202100066

Zhang, D., Li, N., Li, Z.X. and Xie, L. (2020), "Experimental investigation and confinement model of composite confined concrete using steel jacket and prestressed steel hoop", *Constr. Build. Mater.*, **256**(30), 1-13. https://doi.org/10.1016/j.conbuildmat.2020.119399

JK